CrossMark

Needleless electrospinning using sprocket wheel disk spinneret

Usman Ali[1,2,*], Haitao Niu[2], Sarmad Aslam[1,2], Abdul Jabbar[3], Abdul Waqar Rajput[1], and Tong Lin[2]

[1] College of Textile Engineering, BZU, Multan 60800, Pakistan
[2] Institute for Frontier Materials, Deakin University, Geelong, VIC 3216, Australia
[3] Department of Material Engineering, Technical University of Liberec, Studentská 2, Liberec 461 17, Czech Republic

ABSTRACT

Needleless electrospinning is expected to produce nanofibers with a large productivity. In this study, a sprocket wheel disk was used as spinneret to electrospin nanofibers. The sprocket disk shows reliable electrospinning process. In comparison with the conventional disk spinneret, which has no sprocket on the edge, the sprocket wheel produced more uniform nanofibers with smaller fiber diameter. The electric field analysis results indicated that the sprocket wheel generates higher intensity of electric field.

Introduction

Electrospinning has become one of the most effective ways to prepare nanofibers [1, 2]. Electrospun nanofibers membranes have controllable fiber diameter, large surface area-to-volume ratio, high porosity, and excellent air/liquid permeability, which open up huge potential for countless applications [3–6]. The unique amalgamation of these properties has enabled the nanofiber membranes to be applied in diverse areas such as tissue engineering [7, 8], drug release [9–11], energy generation and storage [12–15], filtration [16] chemical engineering, and composite reinforcement [17, 18].

Electrospinning setup conventionally comprises a needle-like fiber generator, a high-voltage power supplier and a collecting electrode [19]. Each needle nozzle normally generates one Taylor cone, and thus has a low fiber productivity, around 0.1–1.0 g h^{-1}. To improve the production rate of nanofibers, a straight forward way is to increase the number of needles [20]. However, there are a number of shortcomings associated with multi-needle electrospinning, such as electric field interruption of neighbor needles, regular cleaning required to avoid clogging, and large space required for installation [21, 22].

Needleless electrospinning has been proved as an efficient solution to improve the nanofiber productivity. Researchers have reported various needleless electrospinning approaches. A key point in needleless electrospinning is to increase the number of polymer Taylor cones in limited solution surface. To increase the number of Taylor cones, mechanisms of different types like bubble electrospinning [23] and magnetic field needleless electrospinning [24] were designed. Their uses enhanced the fiber production significantly but also brought some problems, e.g., complicated electrospinning system, irregular

Address correspondence to E-mail: usman.ali@bzu.edu.pk

🖄 Springer

deposition of fibers on collector and wide diameter distribution of resulting fibers at the same time.

Rotating spinnerets of different geometries like roller [25, 26], metal disk [27], cone [28], and wire electrode [29] were designed and used to produce nanofibers. In 2009, Niu et al. [30] reported a comparison between a cylinder and disk nozzles. They indicated that the main driving force in electrospinning is the intensity of electric field which determines the fiber formation, productivity, and morphology. They also reported that the electric field got more concentrated on the edges of the cylinder than the center surface of the cylinder. This comparison opened a door to shape the geometry of the spinneret. Researchers reported different designs of spinnerets that have a maximum number of edge-like stepped pyramid stage [31, 32], spiral coil [33, 34], plate edge [35], and helix slice spinneret [36]. Liu et al. [37] reported a needle-disk spinneret for generation of multiple jets. Jani et al. [38] reported the use of rotating twisted wire as spinneret to produce nanofibers. These spinnerets have problems with heterogeneous distribution of fiber morphology. Spinneret geometry plays a vital role in fiber formation, fiber morphology, and production rate. Despite the fact that disk has been used as needleless electrospinning fiber generator, it has a very low electric field intensity and poor fiber morphology.

In this study, sprocket wheel was used as a spinneret for electrospinning of nanofibers. The impact of applied voltage, solution concentration, and spinning distance on the morphology of fibers was studied and discussed in details. The sprocket wheel was compared with the disk spinneret in terms of electric field, fibers morphology, and productivity. The electric field intensity around the sprocket wheel is about 50 times higher as compared to the disk.

Experimental

Materials

Polyvinyl alcohol (PVA) was purchased from Daejung chemicals & metals Co. Ltd and used as received. Solutions of different concentrations were made by dissolving PVA powder in water at 70 °C with continuous stirring for 24 h. Deionized water was used as solvent to prepare the solution.

Fabrication of nanofibers

Figure 1a shows the schematic diagram of needleless electrospinning setup. It contains a spinning spinneret (sprocket wheel or disk) as fiber generator, Gamma high-voltage DC power supply, Teflon bath to carry the polymer solution, and metal cylinder as a collector. The dimension of sprocket wheel spinneret is as outer diameter = 60 mm inside diameter = 50 mm, Pitch = 13.10 mm and thickness 5 mm. A 12v DC motor was used to rotate the spinneret. The high potential of 64 kV was applied to the electrospinning solution through inserting a metal electrode connecting the high-voltage output of power supply.
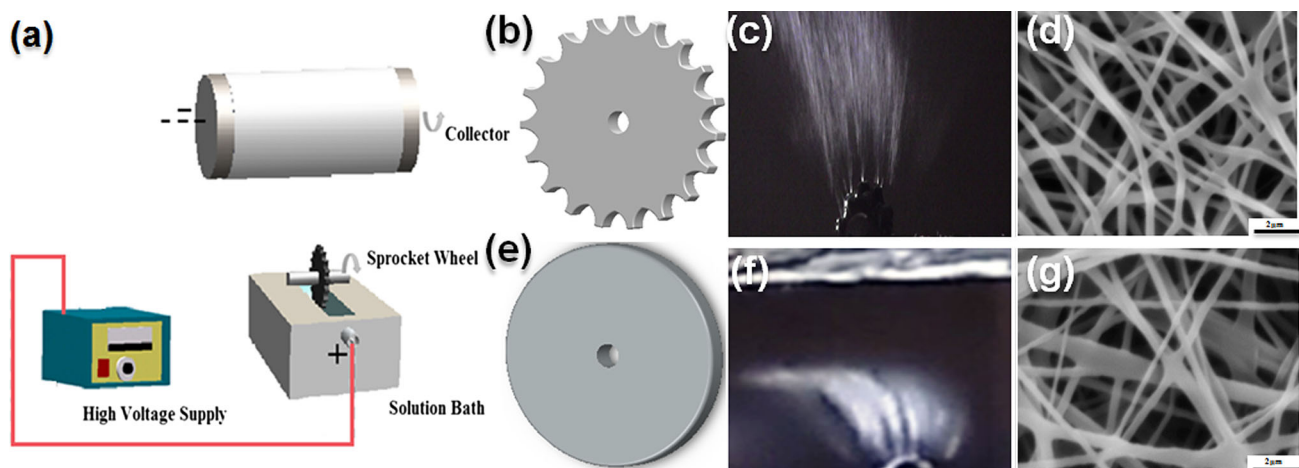
Figure 1 a, b Schematic design of needleless electrospinning setup and diagram of sprocket wheel spinneret, c, d shows the photographs of the sprocket wheel spinning process and SEM image of resulted nanofibers, and e–g shows the diagram, photographs of disk spinning process and SEM image of resulted nanofibers.

The cylinder collector was grounded and covered with aluminum sheet to collect the produced nanofibers at the distance of 13 cm from tip of spinneret.

Characterizations

The fiber morphology was investigated by using scanning electron microscope (JCM-60000Plus NeoScope Benchtop SEM). Image analysis software Image-Pro 6.5 was used to measure the diameters of fibers based on SEM images. SEM samples were chose from different positions of nanofiber membrane, and more than 100 fibers were counted to calculate the average fiber diameter. Electric field simulation was done on the commercial software COMSOL Multiphysics 5.0. The dimensions of the disk spinneret were kept the same as the sprocket wheel spinneret had such as (Diameter = 60 mm and thickness = 5 mm). 3D-shapes of spinnerets were drawn in Solidworks software and then imported into COMSOL Multiphysics 5.0. Photographs and video of the spinning process were recorded by using the digital camera Nikon 5100. The production of nanofibers was calculated by continuously electrospinning for 10 min and then weighting the collected nanofiber membranes with a laboratory weighting balance. All the experiments were conducted at the standard atmospheric conditions, temperature 25 ± 5 °C, and humidity $65 \pm 5\%$.

Results and discussion

Electrospinning and electric field analysis

During electrospinning, a small part of sprocket wheel approximately 25 mm in depth was immersed in PVA solution contained by a Teflon bath. The sprocket wheel was rotated 12 V DC motor supply with a constant speed of 5 rpm. Due to the constant rotation, all the teeth on the sprocket wheel had chances to be immersed into the PVA solution and then brought it up to the top position of sprocket wheel. When the applied voltage was high enough, the electric force overcame the surface tension and generated solution jets from the edges of the teeth as shown in Fig. 1c. The solution jet flew to the collector under the influence of electric field accompanied by the solvent evaporation, as a result dry PVA nanofibers were obtained by the collector. Figure 1d shows

the high-magnification scan electron microscope image of the resulted nanofibers. The formation of interconnections among these nanofibers was due to the large amount production of solution jets and incomplete evaporation of water from solution jets. When these partially dried PVA solution jets were collected and overlapped over each other, the interconnected structure formed.

For comparison, a disk spinneret was also used to produce PVA nanofibers, and the electrospinning process and SEM of resulted PVA nanofibers are shown in Fig. 1f, g, respectively. It was worthwhile to note that the disk spinneret produced coarser PVA nanofibers with larger fiber diameter distribution.

For the better understanding of the sprocket wheel electrospinning process, the electric field intensity of sprocket wheel and disk spinnerets were calculated and compared by finite element method. Figure 2 shows the electric field intensity profile sprocket wheel and disk spinnerets. Although both spinnerets were in a disk-like shape, there was big differences between their electric field intensity profiles. When the spinning distance and applied voltage were kept at 13 cm and 64 kV, respectively, high electric field distributed at the disk edge and remained constant round the disk circumferential direction. For comparison, high electric field only distributed at the teeth of sprocket wheel, with higher intensity 7049 kV/m than that (4693 kV/m) on the disk edge. The calculations of electric field intensity were based on the equation $E = -\nabla V$, (where E is electric field intensity and V is potential); electric field intensity is equal to the negative of the gradient of the potential. Therefore, a geometric shape with large curvature is able to generate high-intensity electric field at the same applied potential. The sprocket spinneret has more protruded teeth (larger curvature) in comparison with a disk spinneret, which enables the sprocket to generate higher intensity electric field than the disk. This could enable sprocket wheel to start eject solution jets at relative lower voltage than disk spinneret and produce finer nanofibers with narrower fiber diameter distribution. This spinneret has higher possibility to be applied for the industrial-scale production of nanofibers.

Jet generation in needleless electrospinning process is a self-initiated process; therefore, the electrospinning parameters, the applied voltage, solution concentration, and spinning distance play crucial roles on the electrospinning process, fiber morphology,

Figure 2 Electric field intensity profiles of **a** sprocket wheel and **b** disk spinneret (spinning distance = 13 cm and applied voltage = 64 kV).
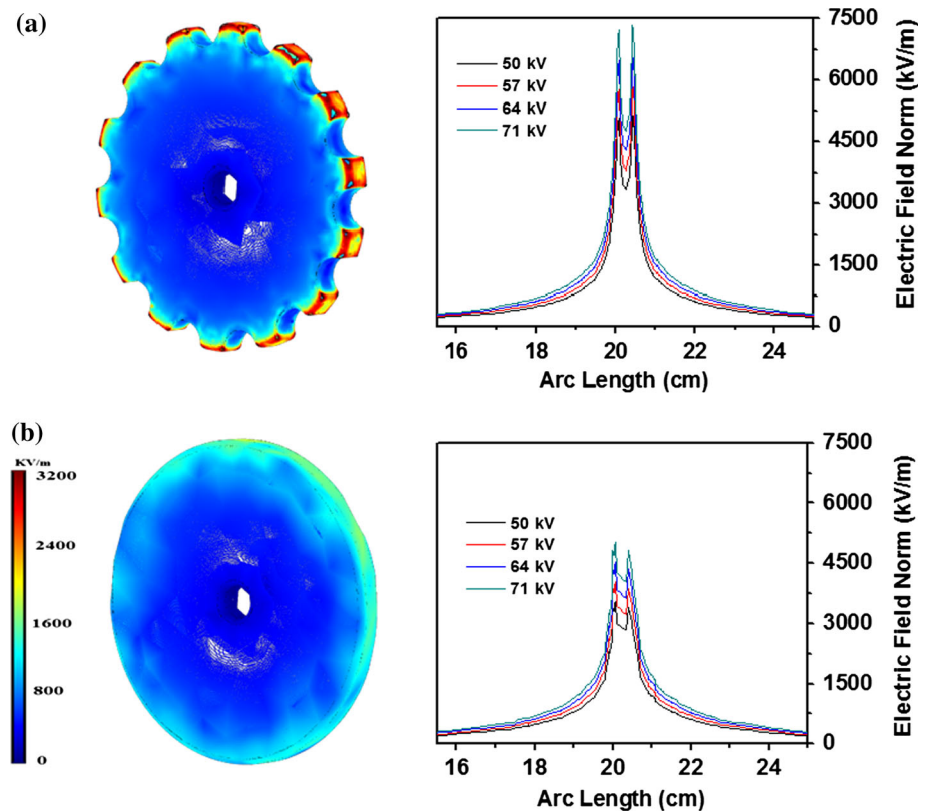
and fiber productivity. In the following sections, the influences of these parameters in sprocket wheel electrospinning will be investigated.

Effect of applied voltage

For the sprocket wheel spinneret, no jet was formed when the applied voltage was lowered than the 38 kV. When the applied voltage was above such a critical voltage, jets started appearing from the edges of the teeth of sprocket wheel, whereas the critical applied voltage to start the jets from the disk spinneret was about 47 kV. Increasing the voltage to 50 kV led to more jets generated from the both spinnerets. To examine the effect of applied voltage on fiber morphology, the applied voltage was increased from 50 to 71 kV, while the spinning distance and solution concentration were fixed at 13 cm and 8 wt%, respectively. Figure 3 shows SEM images of the nanofibers obtained from both the sprocket wheel and disk spinnerets. The sprocket wheel produced finer nanofibers than disk spinneret.

With an increase in the applied voltage, a significant decrease in the average fiber diameter

resulted for both spinnerets (Fig. 4a). As applied voltage was increased from 50 to 71 kV, the average fiber diameter decreased from 426 ± 89 to 285 ± 49 nm for sprocket wheel and it decreased from 495 ± 138 to 385.6 ± 110.2 nm for disk. Higher voltage can provide stronger driving forces, facilitate jet formation, promote solution jet elongation and reduce fiber diameter and standard deviation. At the same applied voltage, the average fiber of nanofibers produced by sprocket wheel was much smaller than that of disk, and with narrower fiber diameter distribution. This is because the intensity of electric field is much higher on the teeth's of sprocket wheel as compared to disk spinneret.

The productivity of nanofibers produced from both the spinnerets at different applied voltage is shown in Fig. 4b, and they both increased with the rising applied voltage. However, the productivity of sprocket was smaller than the disk spinneret although its electric field intensity was much higher as compare to that on the disk spinneret. This is because both spinnerets can produced nanofibers from their circumferences when the

Figure 3 SEM images of electrospun nanofibers by sprocket wheel and disk spinnerets at different applied voltages (spinning distance = 13 cm and solution concentration = 8 wt%).
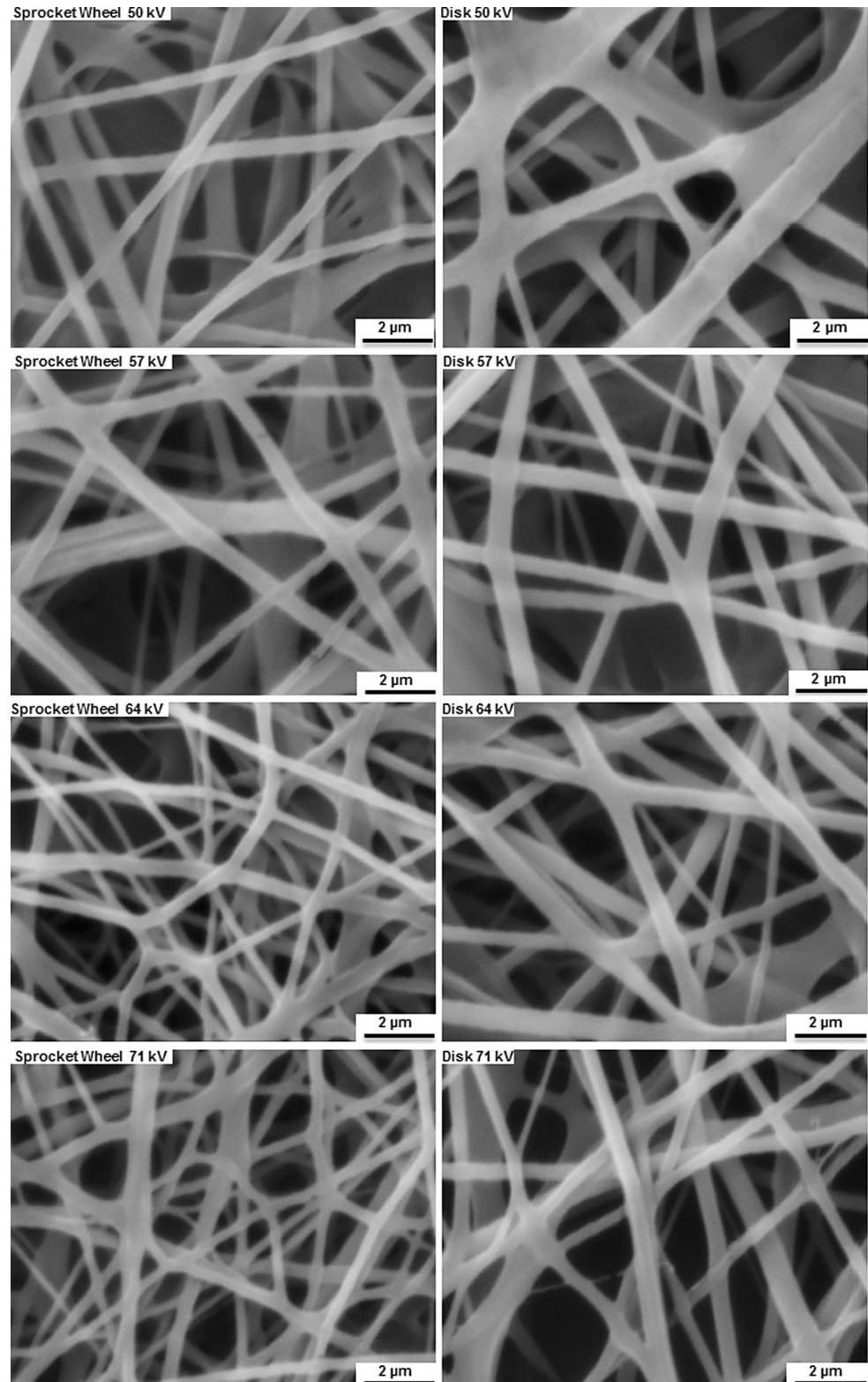
applied voltage was 50 kV, while the disk spinneret utilized all its edge to produced nanofibers sprocket wheel only generated nanofibers on its teeth. The smaller fiber generation area made sprocket wheel produce less than nanofibers than the disk spinneret.

Figure 4 Effect of the applied voltage on **a** average fiber diameter and **b** productivity of nanofibers obtained from sprocket wheel and disk spinnerets (Spinning distance = 13 cm and solution concentration = 8 wt%).
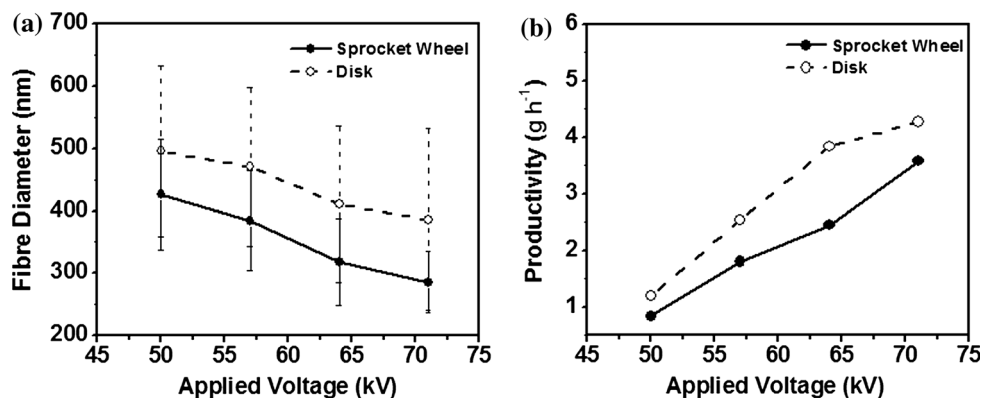
Effect of polymer concentration

Figure 5 shows the SEM images of nanofibers obtained from different concentration solution by both spinnerets. By increasing the solution concentration from 7 to 10 wt%, while fixing the spinning distance and applied voltage at 13 cm and 64 kV, respectively, a significant increase in fiber diameter resulted.

Figure 6a shows the effect of polymer concentration on fiber diameter. For 7 wt% polymer solution, fibers produced by sprocket wheel had a diameter in the range of 164–529 nm. For the fibers produced from disk spinneret, the diameter was coarser, in the range of 321–769 nm. When the concentration was increased to 8 wt%, the diameter changed to 195–722 nm for the sprocket wheel spun fibers and 345–855 nm for the disk spun ones. The increase in the PVA concentration led to stronger cohesive forces between the molecules of the solution and thus preventing the formation of solution jets and fiber drawing and hence resulted in increased fiber diameter. As increasing the solution concentration from 7 to 10 wt%, the average fiber diameter increased from 311 ± 51 nm to 465 ± 135 nm for sprocket wheel and from 463 ± 7 nm to 530 ± 150 nm for disk spinneret. With the increase in solution concentration, the produced nanofibers also showed wider fiber diameter distribution. Because of the high-intensity electric field generated by the sprocket wheel, it always produced finer PVA nanofibers with narrower fiber diameter distribution in comparison with disk spinneret.

Figure 6b shows the impact of solution concentration on the productivity of nanofibers obtained from both the spinnerets. With the increase in the solution concentration from 7 to 10 wt%, the fiber productivity of sprocket wheel and disk spinnerets increased from 2.09 to 4.45 g h^{-1} and from 2.75 to 5.24 g h^{-1}, respectively. This increase in productivity is due to the growing solid PVA content in the higher concentration solutions, which produced solution jets with more PVA macromolecules inside, as a result the obtained nanofibers had larger fiber diameter with improved fiber yield.
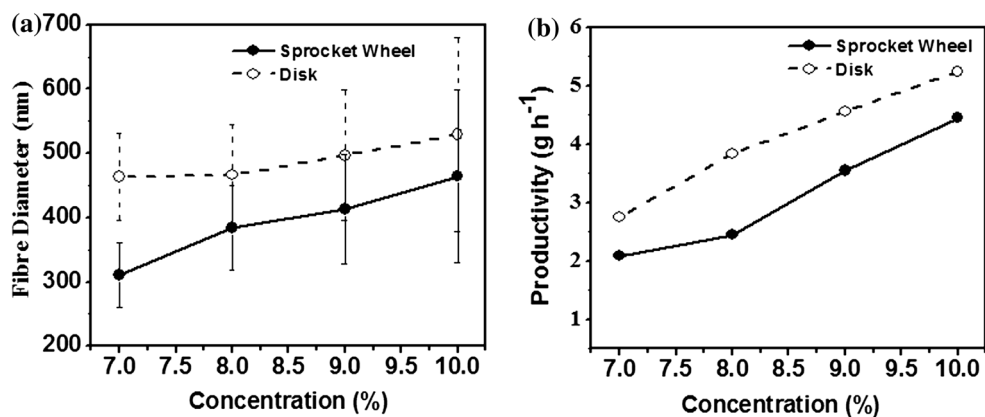
Effect of spinning distance

The impact of spinning distance on the morphology of nanofibers was also examined by changing the spinning distance between 11 and 15 cm, with fixed applied voltage at 64 kV and polymer solution concentration at 8 wt%. Figure 7 shows the SEM images of nanofibers obtained from different spinning distances. Increasing the spinning distance had slight influence on reducing the fiber diameter. As shown in Fig. 8a, when the spinning distance was 11 cm the average fiber diameter was 403 ± 78 nm for sprocket wheel and 497 ± 137 nm for disk spinneret. With the increase in the spinning distance to 13 cm, the diameter fall down and further increasing the spinning distance to 15 cm leads the average fiber diameter to 356 ± 86 nm for sprocket wheel and 429 ± 114 nm for disk spinneret. The increase in the spinning distance led to the decrease in electric field intensity, but it facilitated the jet to be stretched more and hence resulting in slight decrease in the fiber diameter.

Figure 8b shows the impact of spinning distance on the productivity of nanofibers obtained from both the spinnerets. It was found that with the increase in the spinning distance resulted in reduced fiber productivity for both the spinnerets. With the increase in the spinning distance from 11 to 15 cm, the
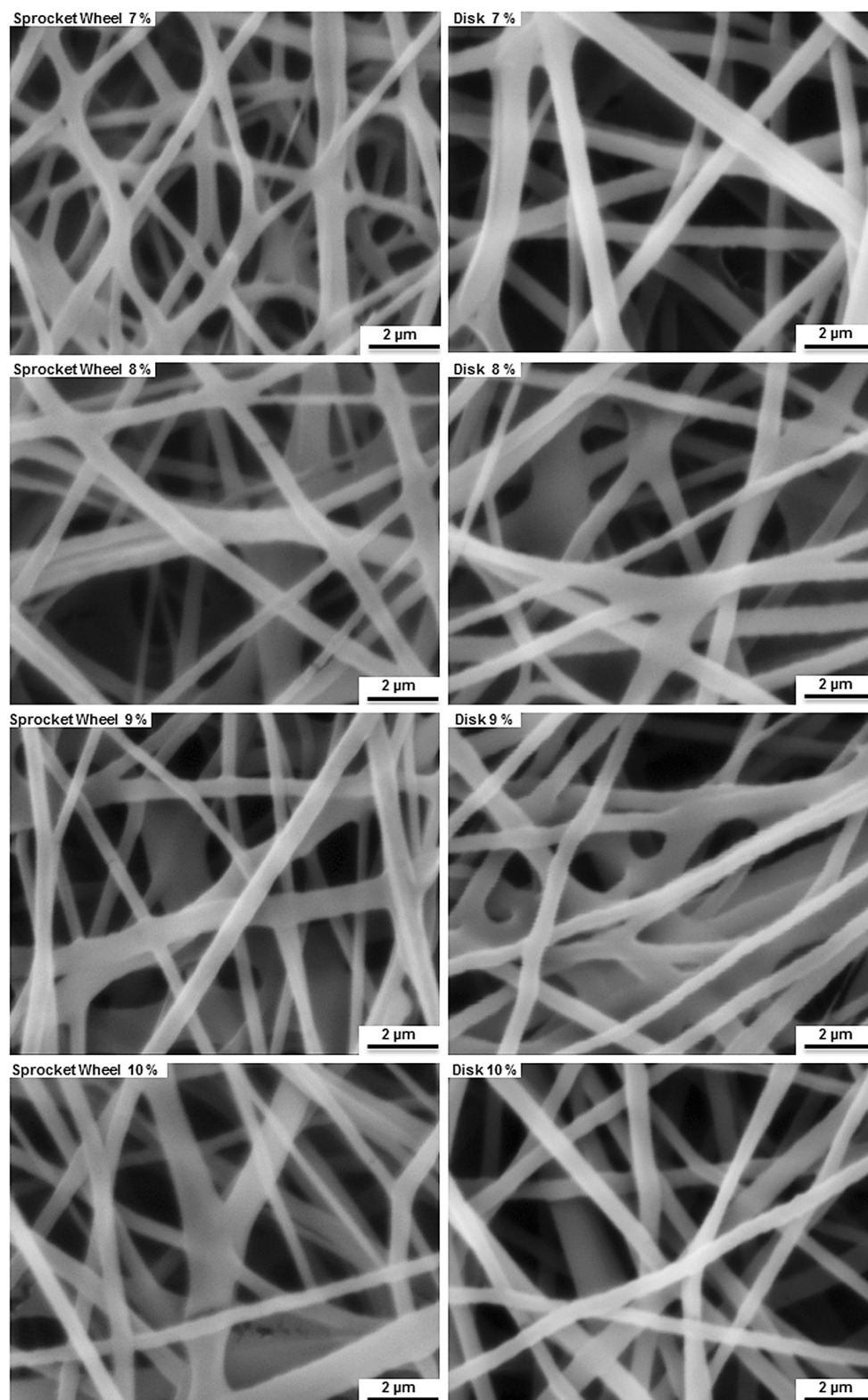
Figure 5 SEM images of electrospun nanofibers from sprocket when and disk spinneret with different PVA concentrations (spinning distance = 13 cm and applied voltage = 64 kV).

Figure 6 Effect of polymer concentration on **a** average fiber diameter and **b** productivity of nanofibers from sprocket wheel and disk spinneret (Applied voltage = 64 kV and spinning distance = 13 cm).
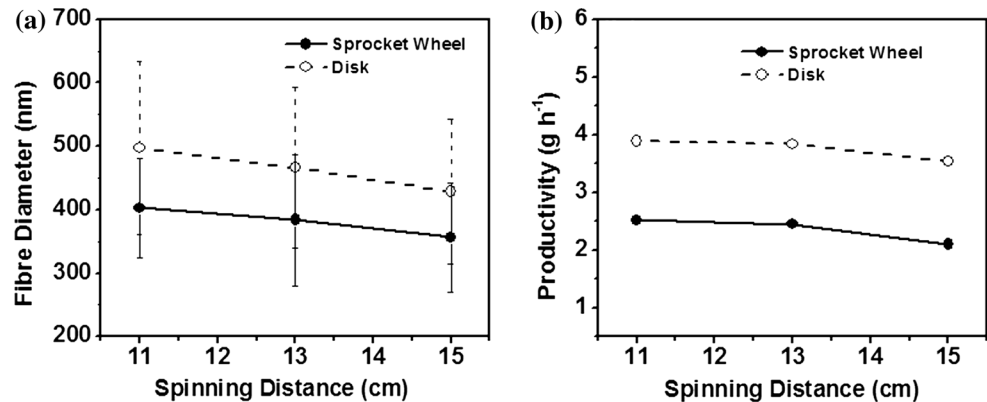

Figure 7 SEM Photos of electrospun nanofibers from sprocket wheel and disk spinneret at different spinning distances. (PVA concentration = 8 wt% and applied voltage = 64 kV).
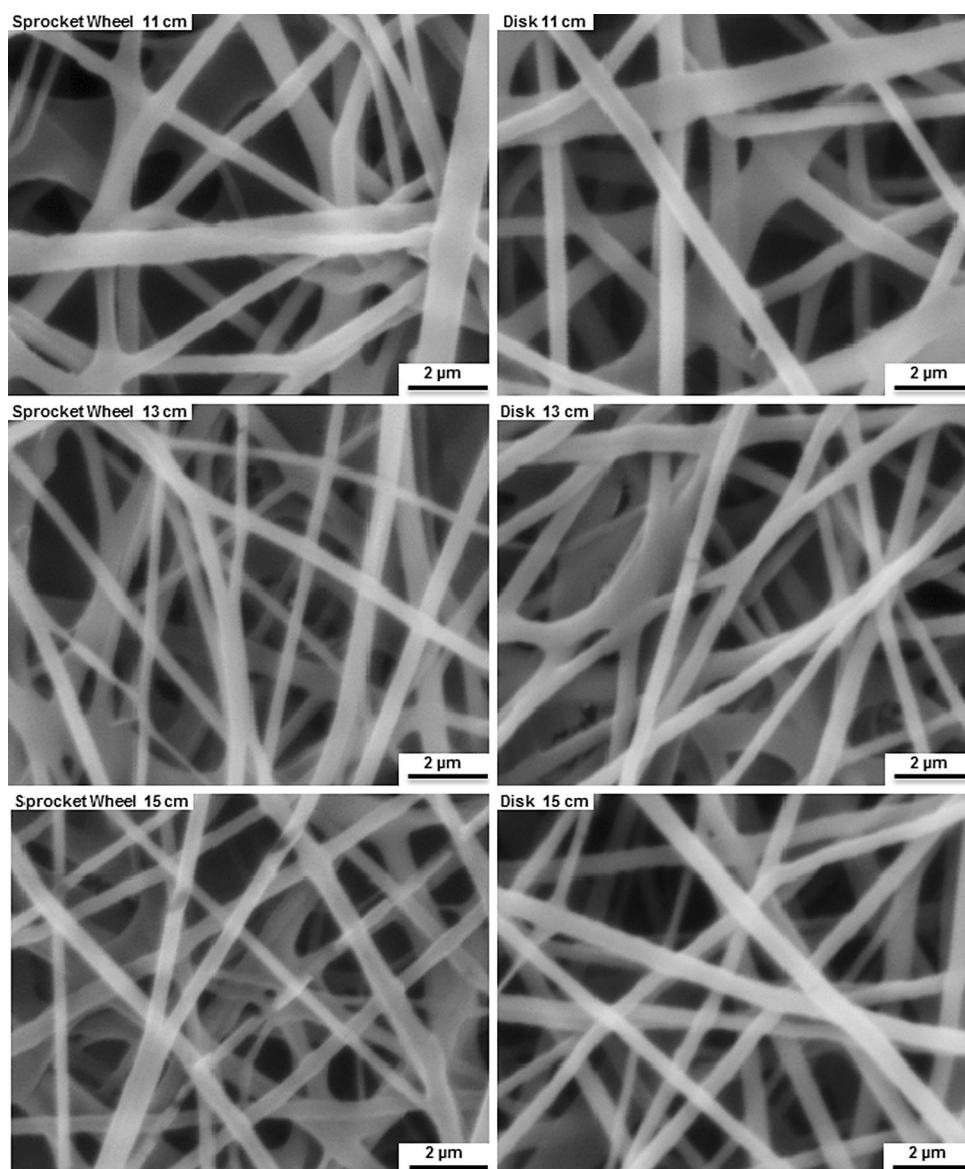
Figure 8 Impact of spinning distance on **a** average fiber diameter and **b** productivity of nanofibers from sprocket wheel and disk spinneret. (PVA concentration 8 wt% and applied voltage 64 kV).

productivity of fibers decreased from 2.52 to 2.1 g h^{-1} for sprocket wheel and from 3.89 to 3.54 g h^{-1} for disk spinneret. This decrease in production is due to the decrease in electric field intensity on the spinneret that leads to less jet generation from the spinneret and secondly due to the formation of finer fibers due to extra stretching. Sprocket wheel also produced finer nanofibers with lower fiber productivity. Although this sprocket wheel had smaller fiber yield, we believed that it can be improved in the future work by optimizing the area ratio between teeth and sag of sprocket wheel by improving the area of teeth to increase the electrospinning area.

Conclusion

We have proved that sprocket wheel spinneret can be used as a spinneret to electrospin polymer solution into nanofibers. This spinneret was compared with the disk spinneret in terms of critical voltage for electrospinning, electric field intensity, produced nanofiber diameter, and fiber productivity. Higher electric filed intensity is formed on the teeth of sprocket wheel that that on the edge of disk spinneret. The generated high-intensity electric field by the sprocket wheel spinneret enables it to start electrospinning at a relative low applied voltage, produce much finer nanofibers than the disk spinneret. This novel generator may be useful for the production of nanofibers on industrial scales.

Acknowledgements

References

[1] Sahay R, Parveen H, Baji A, Ganesh VA, Ranganath AS (2017) Fabrication of PVDF hierarchical fibrillar structures using electrospinning for dry-adhesive applications. J Mater Sci 52:2435–2441. doi:10.1007/s10853-016-0537-9

[2] Cai Y, Gevelber M (2017) Analysis of bending region physics in determining electrospun fiber diameter: effect of relative humidity on evaporation and force balance. J Mater Sci 52:2605–2627. doi:10.1007/s10853-016-0553-9

[3] Sanfelice RC, Mercante LA, Pavinatto A, Tomazio NB, Mendonça CR, Ribeiro SJL et al (2017) Hybrid composite material based on polythiophene derivative nanofibers modified with gold nanoparticles for optoelectronics applications. J Mater Sci 52:1919–1929. doi:10.1007/s10853-016-0481-8

[4] Panthi G, Park S-J, Kim T-W, Chung H-J, Hong S-T, Park M et al (2015) Electrospun composite nanofibers of polyacrylonitrile and Ag2CO3 nanoparticles for visible light photocatalysis and antibacterial applications. J Mater Sci 50:4477–4485. doi:10.1007/s10853-015-8995-z

[5] Chiscan O, Dumitru I, Tura V, Stancu A (2012) PVC/Fe electrospun nanofibers for high frequency applications. J Mater Sci 47:2322–2327. doi:10.1007/s10853-011-6047-x

[6] Zhang L, Aboagye A, Kelkar A, Lai C, Fong H (2014) A review: carbon nanofibers from electrospun polyacrylonitrile and their applications. J Mater Sci 49:463–480. doi:10.1007/s10853-013-7705-y

[7] Van Hong Thien D, Hsiao SW, Ho MH, Li CH, Shih JL (2013) Electrospun chitosan/hydroxyapatite nanofibers for bone tissue engineering. J Mater Sci 48:1640–1645. doi:10.1007/s10853-012-6921-1

[8] Jing X, Jin E, Mi H-Y, Li W-J, Peng X-F, Turng L-S (2015) Hierarchically decorated electrospun poly(ε-caprolactone)/nanohydroxyapatite composite nanofibers for bone

tissue engineering. J Mater Sci 50:4174–4186. doi:10.1007/s10853-015-8933-0

[9] Zahedi P, Rezaeian I, Jafari SH (2013) In vitro and in vivo evaluations of phenytoin sodium-loaded electrospun PVA, PCL, and their hybrid nanofibrous mats for use as active wound dressings. J Mater Sci 48:3147–3159. doi:10.1007/s10853-012-7092-9

[10] Ramakrishna S, Jose R, Archana PS, Nair AS, Balamurugan R, Venugopal J et al (2010) Science and engineering of electrospun nanofibers for advances in clean energy, water filtration, and regenerative medicine. J Mater Sci 45:6283–6312. doi:10.1007/s10853-010-4509-1

[11] Goh Y-F, Shakir I, Hussain R (2013) Electrospun fibers for tissue engineering, drug delivery, and wound dressing. J Mater Sci 48:3027–3054. doi:10.1007/s10853-013-7145-8

[12] Fang J, Niu H, Wang H, Wang X, Lin T (2013) Enhanced mechanical energy harvesting using needleless electrospun poly(vinylidene fluoride) nanofibre webs. Energy Environ Sci 6:2196–2202

[13] Peng S, Li L, Lee JKY, Tian L, Srinivasan M, Adams S et al (2016) Electrospun carbon nanofibers and their hybrid composites as advanced materials for energy conversion and storage. Nano Energy 22:361–395

[14] Zhang B, Kang F, Tarascon J-M, Kim J-K (2016) Recent advances in electrospun carbon nanofibers and their application in electrochemical energy storage. Progress Mater Sci 76:319–380

[15] Wang J, Yang G, Wang L, Yan W (2016) Fabrication of one-dimensional CdFe2O4 yolk/shell flat nanotubes as a high-performance anode for lithium-ion batteries. J Mater Sci, pp 1–13, doi: 10.1007/s10853-016-0672-3

[16] Qin X, Subianto S (2017) 17 - Electrospun nanofibers for filtration applications A2 - Afshari, Mehdi. In: Electrospun nanofibers, ed, Woodhead Publishing, p 449–466

[17] Ortenzi MA, Basilissi L, Farina H, Di Silvestro G, Piergiovanni L, Mascheroni E (2015) Evaluation of crystallinity and gas barrier properties of films obtained from PLA nanocomposites synthesized via "in situ" polymerization of l-lactide with silane-modified nanosilica and montmorillonite. Eur Polym J 66:478–491

[18] Neppalli R, Causin V, Benetti EM, Ray SS, Esposito A, Wanjale S et al (2014) Polystyrene/TiO2 composite electrospun fibers as fillers for poly(butylene succinate-co-adipate): structure, morphology and properties. Eur Polym J 50:78–86

[19] Wang L, Ryan AJ (2011) Introduction to electrospinning. In: Bosworth LA, Downes S (eds) Electrospinning for tissue regeneration. Woodhead Publishing, Oxford, pp 3–33

[20] Wang S, Yang Y, Zhang Y, Fei X, Zhou C, Zhang Y et al (2014) Fabrication of large-scale superhydrophobic composite films with enhanced tensile properties by multi-nozzle conveyor belt electrospinning. J Appl Polym Sci 131:39735. doi:10.1002/app.39735

[21] Angammana CJ, Jayaram SH (2011) The effects of electric field on the multijet electrospinning process and fiber morphology. Ind Appl IEEE Trans 47:1028–1035

[22] Kumar A, Wei M, Barry C, Chen J, Mead J (2010) Controlling fiber repulsion in multijet electrospinning for higher throughput. Macromol Mater Eng 295:701–708

[23] Liu Y, He JH (2007) Bubble electrospinning for mass production of nanofibers. In: International journal of nonlinear sciences and numerical simulation 8, ed, p 393

[24] Niu H, Lin T (2012) Fiber generators in needleless electrospinning. J Nanomater 2012:1–13

[25] Yalcinkaya F, Yalcinkaya B, Jirsak O (2016) Analysis of the effects of rotating roller speed on a roller electrospinning system. Text Res J. doi:10.1177/0040517516641362

[26] Yalcinkaya B, Callioglu FC, Yener F (2014) Measurement and analysis of jet current and jet life in roller electrospinning of polyurethane. Text Res J 84:1720–1728

[27] Wei L, Yu H, Jia L, X (2016) Qin High-throughput nanofiber produced by needleless electrospinning using a metal dish as the spinneret. Text Res J. doi:10.1177/0040517516677232

[28] Lu B, Wang Y, Liu Y, Duan H, Zhou J, Zhang Z et al (2010) Superhigh-throughput needleless electrospinning using a rotary cone as spinneret. Small 6:1612–1616

[29] Bhattacharyya I, Molaro MC, Braatz RD, Rutledge GC (2016) Free surface electrospinning of aqueous polymer solutions from a wire electrode. Chem Eng J 289:203–211

[30] Niu H, Lin T, Wang X (2009) Needleless electrospinning. I. A comparison of cylinder and disk nozzles. J Appl Polym Sci 114:3524–3530

[31] Jiang G, Zhang S, Qin X (2014) Effect of processing parameters on free surface electrospinning from a stepped pyramid stage. J Ind Text 45(4):483–494

[32] Jiang G, Qin X (2014) An improved free surface electrospinning for high throughput manufacturing of core–shell nanofibers. Mater Lett 128:259–262

[33] Wang X, Niu H, Wang X, Lin T (2012) Needleless electrospinning of uniform nanofibers using spiral coil spinnerets. J Nanomater 2012:1–9

[34] Wang X, Wang X, Lin T (2012) Electric field analysis of spinneret design for needleless electrospinning of nanofibers. J Mater Res 27:3013–3019

[35] Thoppey NM, Bochinski JR, Clarke LI, Gorga RE (2010) Unconfined fluid electrospun into high quality nanofibers from a plate edge. Polymer 51:4928–4936

[36] Lu W, Ma M, Xu H, Zhang B, Cao X, Guo Y (2015) Gelatin nanofibers prepared by spiral-electrospinning and cross-linked by vapor and liquid-phase glutaraldehyde. Mater Lett 140:1–4

[37] Liu Z, Chen R, He J (2016) Active generation of multiple jets for producing nanofibres with high quality and high throughput. Mater Des 94:496–501

[38] Jani H, Toni P, Eero S, Mikko R (2015) Needleless electrospinning with twisted wire spinneret. Nanotechnology 26:025301